Smart Mater. Struct. **16** (2007) 1164–1170 doi:10.1088/0964-1726/16/4/026

Numerical assessment of the methods of measurement of the electrical resistance in carbon fiber reinforced cement

Sirong Zhu[1] **and D D L Chung**[2]

Composite Materials Research Laboratory, University at Buffalo, State University of New York, Buffalo, NY 14260-4400, USA

E-mail: ddlchung@buffalo.edu

Received 26 September 2006, in final form 19 April 2007
Published 25 June 2007
Online at stacks.iop.org/SMS/16/1164

Abstract
Carbon fiber reinforced cement is a smart material due to its sensing ability, which is based on piezoresistivity. A finite element model for simulating the measurement of electrical resistance in this material is provided. The measured four-probe resistance decreases with increasing distance between the adjacent voltage and current contacts. For a beam of size $320 \times 40 \times 40$ mm^3, the minimum distance for accurate four-probe resistivity measurement is 5 mm for surface contacts (at the end surfaces), 5 mm for loop contacts (around the perimeter) and 40 mm for line contacts (on one surface). The two-probe resistivity is most inaccurate for the line contacts. For loop contacts, the two-probe resistivity is accurate when the aspect ratio exceeds 8, and the four-probe resistivity is accurate when the aspect ratio exceeds 1.5. For a column of size $426 \times 92 \times 76$ mm^3, the minimum distance between the adjacent current and voltage contacts for accurate four-probe resistivity measurement is 50 mm for loop contacts and 400 mm for line contacts. For a slab of size $9.75 \times 4.88 \times 0.30$ m^3, the minimum distance for accurate four-probe resistivity measurement along the 9.75 m length is 250 mm for line contacts.

1. Introduction

Cement-based materials are the dominant construction materials for infrastructures. By the use of short conductive fibers, such as carbon fibers, as an admixture, the electrical resistivity of the resulting cement-based material can be significantly decreased, particularly if the fiber volume fraction exceeds the percolation threshold [1, 2]. The conductivity enables multifunctionality, so that the material is more than just a structural material [3]. One of the nonstructural functions is the sensing of strain, as made possible by piezoresistivity, i.e. the reversible effect of strain on the electrical resistivity [4–11]. Strain sensing relates to stress sensing and is valuable for traffic monitoring [12], border monitoring, building security, building facility management (through the use of the occupancy of each room to control the lighting, heating, cooling and ventilation of the room for the purpose of saving energy), truck weighing and structural vibration control. Another nonstructural function relates to the use of a structural material as a heating element that is based on resistance (Joule) heating [13–16]. Heating applications include the deicing of airport runways and bridges and the heating of building floors. Yet another nonstructural application relates to the use of a conductive cement-based material as an electrical contact for implementing cathodic protection [17], which is a method of corrosion protection of steel reinforcing bars (rebars) embedded in concrete. All these functions hinge on the electrical conductivity of the cement-based material. Cement reinforced with a small proportion of short carbon fibers of diameters around 15 μm has been shown to be effective for all of the functions mentioned above [2].

For strain sensing, the electrical resistance of the cement-based material needs to be measured accurately. For the applications related to heating and cathodic protection, the electrical resistance of the cement-based material needs to be

[1] Permanent address: Department of Engineering Structures and Mechanics, School of Science, Wuhan University of Technology, Wuhan, Hubei 430070, People's Republic of China.
[2] Author to whom any correspondence should be addressed.

measured for the purpose designing the heating element or the electrical contact for cathodic protection. Thus, all of these applications require at some point the measurement of the electrical resistance.

The method of electrical resistance measurement of a material is conceptually simple, as it is based on Ohm's law. However, it is partly complicated by the electrical resistance that is associated with the electrical contacts that are used for making the measurement. Such contact resistance is to be distinguished from the resistance of the material under investigation. To circumvent this problem, the four-probe method [18] is used. In this method, four electrical contacts are used; the outer two are for passing current, while the inner two are for measuring the voltage. The voltage divided by the current gives the resistance of the portion of the specimen between the inner contacts. In contrast, the two-probe method uses only two electrical contacts, so that each contact is both for passing current and for voltage measurement. As a consequence, the resistance obtained by using the two-probe method has the contact resistance included in it, whereas that obtained by using the four-probe method essentially does not include the contact resistance. Another complication relates to the positions and geometry of the electrical contacts, as they affect the extent of uniformity of the current density in the region of resistance measurement.

Due to the large sizes and various geometries of concrete structures, the electrical contact configuration may have to deviate from the ideal case. For example, the two-probe method may be easier to implement than the four-probe method. As another example, the measurement of the surface resistance (using a surface current, as provided by electrical contacts that are on the same surface) may be easier to implement than the measurement of the volume resistance (using electrical contacts that ideally allow a uniform current density distribution throughout the volume of resistance measurement). As yet another example, the measurement of the volume resistance using current contacts that are around the perimeter in planes that are perpendicular to the direction of resistance measurement may be easier to implement than that using current contacts that are at the two end surfaces.

For the purpose of implementation, it is important to assess the various methods of resistance measurement, including those that are not ideal. This assessment can be conducted experimentally, but it can also be done numerically. The numerical method is attractive in that it can be applied to various sizes and geometries. In contrast, the experimental method can only be applied to a limited number of sizes and geometries and, moreover, it tends to be difficult when the specimen is large or heavy. Prior work has provided a degree of experimental assessment for carbon fiber reinforced cement [18], but there is no prior work on numerical assessment for any cement-based material. Therefore, this paper is aimed at numerical simulation of the measurement of electrical resistance in carbon fiber reinforced cement.

The objectives of this paper are to assess numerically the effectiveness of various electrical contact configurations for measuring the electrical resistivity of carbon fiber reinforced cement and to provide a numerical tool for design of the contact configurations for various specimen geometries and dimensions.

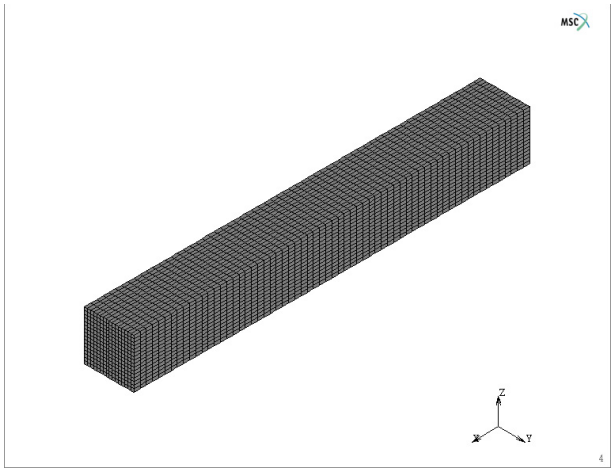

Figure 1. Meshed beam in the finite element model.

2. Method of simulation

The carbon fiber reinforced cement is supposed to be isotropic and homogeneous. When the carbon fiber content is 0.5 vol% (just below the percolation threshold [1]), the volume electrical resistivity is 1.2×10^4 Ω cm [18], which is low compared to the value of 5×10^5 Ω cm for the case without fiber [19].

The simulation involves the use of the finite element method (FEM), as conducted for a beam, a slab and a column. A commercially available FEM tool called MARC is used. Figure 1 shows the finite element mesh for a beam of size $320 \times 40 \times 40$ mm^3. The specimen is divided into 16 384 solid elements in the FEM analysis. The calculation module of MARC called 'Joule heating' is used to calculate the steady-state electric field distribution.

In the case of a beam-shaped specimen, the resistance is measured along the length of the beam. Three electrical contact configurations are assessed, as listed below and illustrated in figure 2.

(a) Surface contacts: electrical contacts for passing current are at the ends of the specimen, such that each contact covers the entire end surface.
(b) Loop contacts: electrical contacts for passing current are around the perimeter at the ends of the specimen.
(c) Line contacts: electrical contacts for passing current are on the top surface at the ends of the specimen.

The contact resistance is associated with (i) the resistance of the interface between the electrical contact and the specimen surface and (ii) the resistance within the contact material. Since the contact material is a metal of high conductivity (such as silver from silver paint), the interfacial resistance ((i) above) is expected to dominate the contact resistance.

In the FEM simulation, the resistance of an electrical contact is considered as the additional resistance of the elements that line the interface between the electrical contact and the specimen. In other words, the resistivity of the contact elements is effectively higher than that of the other elements in the specimen. The effective resistivity of the contact elements is obtained numerically by applying the model to calculate (i) the resistance for the unreal case of zero contact resistance

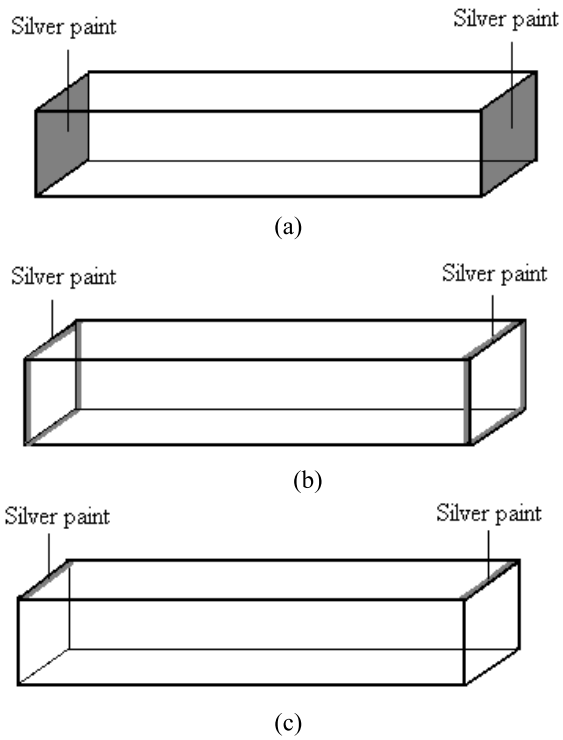

Figure 2. Electrical contact configurations. (a) Surface contacts; (b) loop contacts; (c) line contacts.

and (ii) the resistance for the real case corresponding to a value of the contact resistance that is based on experimental determination (as described below [18]). The difference between the two calculated resistances is $2R_c$, where R_c is the resistance due to one electrical contact. The use of two current contacts results in a total contact resistance of $2R_c$.

The contact resistivity is the product of R_c and B, where B is the area of the interface between the electrical contact and the specimen surface. In the case of surface contacts (figure 2(a)), B is the area of the specimen perpendicular to the direction of resistance measurement. In the case of loop (figure 2(b)) and line (figure 2(c)) contacts, B is much smaller. In this work, we assume that the width of the loop and line contacts is 1 mm.

For the case of electrical contacts in the form of silver paint loops, the contact resistivity is 6×10^3 Ω cm^2, as calculated from the experimentally measured values of the two-probe and four-probe resistances [18]. In this calculation, we assume that the loop is 1 mm wide. Furthermore, we note that the difference between the two-probe resistance (two-probe resistivity 1.53×10^4 Ω cm multiplied by the length of the specimen between the contacts and divided by the area of the specimen perpendicular to the direction of resistance measurement) and the four-probe resistance (four-probe resistivity 1.32×10^4 Ω cm multiplied by the length of the specimen between the voltage contacts and divided by the area of the specimen perpendicular to the direction of resistance measurement) is equal to $2R_c$.

By using the contact resistivity of 6×10^3 Ω cm^2 and B values of 1600, 160 and 40 mm^2, respectively, for the surface, loop and line contacts of this work (figure 2), we obtain corresponding R_c values of 390, 3900 and 15 800 Ω.

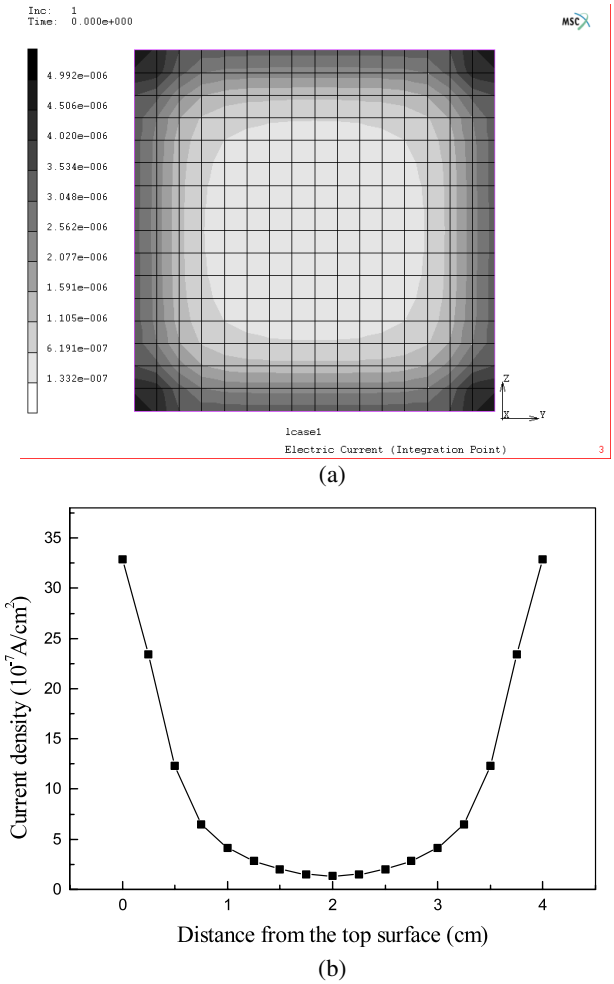

Figure 3. Current density distribution for the case of the loop contacts of figure 2(b). In (a), the current density is in A cm^{-2}.

3. Results and discussion

3.1. Current density distribution in a beam

This section pertains to calculation of the current density distribution in a beam-shaped specimen of size 320 × 40 × 40 mm^3.

Different configurations for the current contacts (figure 2) result in different current density distributions in the specimen. This in turn results in different values of the measured resistance, since the measured resistance is obtained by dividing the measured voltage by the applied current. The applied current is considered to be 0.1 μA, which is typical for the measurement of the resistance of carbon fiber reinforced cement.

The current density distribution is uniform throughout the end surface for the case of the surface contacts of figure 2(a). Figures 3 and 4 show the non-uniform current density distribution at the end surface for the configurations of figures 2(b) and (c), respectively. Figure 3 shows that, for the case of the loop contacts of figure 2(b), the current density is highest at the boundary of the specimen cross section and decreases toward the center of the cross section. Figure 4 shows that, for the case of the line contacts of figure 2(c), the

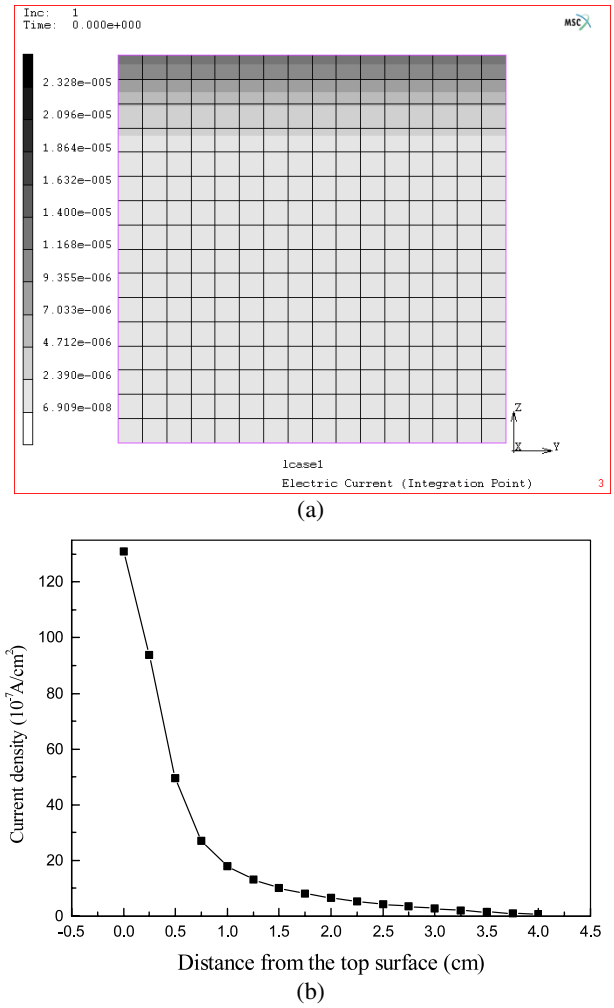

Figure 4. Current density distribution for the case of the line contacts of figure 2(c). In (a), the current density is in A cm^{-2}.

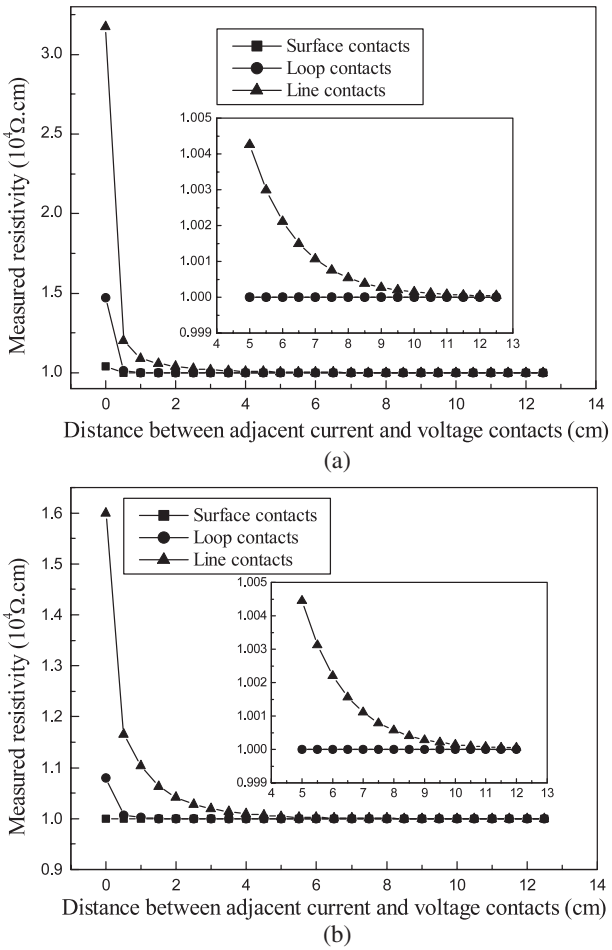

Figure 5. Dependence of the measured resistivity (ρ_o in equation (1)) of the beam-shaped specimen obtained by simulation on the distance between the adjacent voltage and current contacts. The inset shows the expanded view of the graph beyond 5 cm in the horizontal scale. (a) The real case with the contact resistance taken into account. (b) The unreal case with the contact resistance not taken into account.

current density is highest at the top surface and monotonically decreases as the distance from the top surface increases.

3.2. Measured resistance of a beam

This section pertains to calculation of the measured resistance in a beam-shaped specimen of size 320 × 40 × 40 mm^3. As in section 3.1, the specimen is divided into 16 384 elements in the FEM analysis.

In the procedure of electrical resistance measurement, the volume resistance of the part of the specimen between the voltage contacts (the same as the current contacts in the case of the two-probe method) is obtained by dividing the measured voltage between the voltage contacts by the applied current. In the four-probe method, the voltage contacts are separate from the current contacts. In the case of the configurations of figures 2(b) and (c), the distance between the adjacent voltage and current contacts can affect the degree of uniformity of the current density distribution in the part of the specimen between the voltage contacts. This is because the current is injected from the perimeter (figure 2(b)) or the top surface (figure 2(c)) and, as a consequence, the current does not penetrate the entire cross section at the point of injection. A uniform current density is necessary for accurate measurement of the resistivity. Due to the non-uniformity, the measured resistivity deviates from the accurate value. In this section, the measured resistivity is determined numerically for each of the configurations of figure 2 and for various distances between the adjacent voltage and current contacts in each case. A distance of zero corresponds to the two-probe method. All non-zero distances correspond to the four-probe method. The voltage contacts are not shown in figure 2. However, in the simulation, each voltage contact is at the center point of a line on the top surface in the direction perpendicular to the direction of resistance measurement.

Figure 5 shows the measured resistivity obtained numerically for the case with and without contact resistance. The case with the contact resistance corresponds to reality. Although the case without contact resistance is not reality, it is useful for helping distinguish between the effect of the contact resistance and the effect of non-uniform current density distribution. The case with contact resistance reflects both effects, whereas the case without contact resistance reflects

only the effect of non-uniform current density distribution. The method of accounting for the contact resistance numerically is explained in section 2.

For all of the three electrical contact configurations of figure 2, the measured resistivity for the case with contact resistance (figure 5(a)) decreases monotonically with increasing distance between the adjacent voltage and current contacts. This partly means that the four-probe method is more accurate than the two-probe method. In the case of the surface contacts of figure 2(a), this trend is because of the contact resistance only, as the current is uniformly injected throughout the cross section from the end surface. In the case of the loop contacts of figure 2(b) and the line contacts of figure 2(c), this trend is partly due to the contact resistance and partly due to the non-uniform current injection. The greater is this distance, the more uniform is the current density distribution, and the more accurate is the measured resistivity. The minimum distance between adjacent voltage and current contacts for accurate resistivity measurement is 5 mm in the case of surface and loop contacts, and is 40 mm in the case of line contacts, as shown in figure 5(a).

For a distance of zero, which corresponds to the two-probe method, the measured resistivity is highest (least accurate) for the line contacts, less high for the loop contacts and lowest (most accurate) for the surface contacts, as shown in figure 5(a). This is due to the most severe current density non-uniformity for the case of the line contacts, as shown in figure 4.

The curves for surface and loop contacts in figure 5(a) are close, whereas the curve for line contacts is different. This implies that the use of loop contacts is essentially as reliable as the use of surface contacts. This is consistent with experimental results [18]. On the other hand, the use of line contacts is not reliable, unless the distance between the voltage and current contacts exceeds 40 mm.

For the unreal case of figure 5(b) (without contact resistance), the measured resistivity using surface contacts is independent of the distance between the adjacent voltage and current contacts and the value is the same for two-probe and four-probe methods. This is expected, since the contact resistance is the only cause of the decrease in measured resistivity with increasing distance for the case with surface contacts in figure 5(a) (with contact resistance). For a distance of zero, the measured resistivity is higher in figure 5(a) than in 5(b), whether surface, loop or line contacts are used. This is expected, since figure 5(a) accounts for the contact resistance, whereas figure 5(b) does not. The minimum distance for the measured resistivity to decrease to the accurate value is essentially the same in figures 5(a) and (b), whether loop or line contacts are used. This means that the minimum distance shown by figure 5(a) for loop and line contacts mainly reflects the non-uniformity in the current density distribution rather than reflecting the contact resistance.

In the simulation, we input the resistivity (referred to as the input resistivity ρ_i) of 1.0×10^4 Ω cm, which is close to the previously reported experimental value of 1.2×10^4 Ω cm [18]. Figure 5 shows that the calculated resistivity (referred to as the output resistivity ρ_o) is higher than the input resistivity when the adjacent current and voltage contacts are close, and is close to the input resistivity when the distance between the adjacent current and voltage contacts is large. This can be explained by noting that the measured resistance R is related to ρ_i and ρ_o by

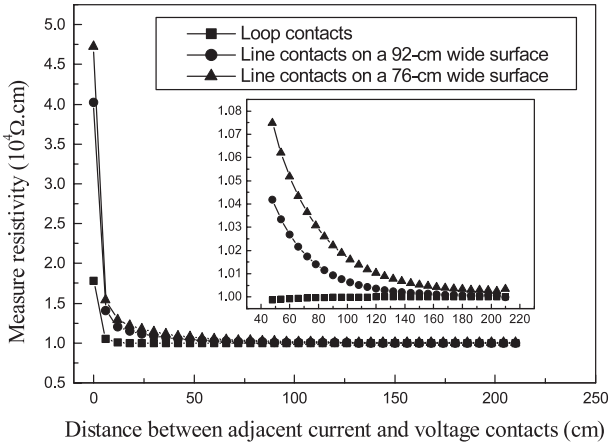

Figure 6. Dependence of the measured resistivity of a column obtained by simulation on the distance between the adjacent voltage and current contacts. The inset shows the expanded view of the graph beyond about 50 cm in the horizontal scale.

$$R = \frac{\rho_i l}{A_i} = \frac{\rho_o l}{A_o}, \tag{1}$$

where A_i is the input area, which is the part of the cross-sectional area through which current actually passes, and A_o is the output area, which is the total cross-sectional area of the beam. In other words, the output resistivity is the measured resistivity, which is calculated from the measured resistance by taking the total cross-sectional area into account, even though the current penetration may not be complete.

Based on equation (1),

$$\rho_o = \frac{A_o}{A_i}\rho_i. \tag{2}$$

Because $A_o \geqslant A_i$, $\rho_o \geqslant \rho_i$.

3.3. Measured resistance of a column

This section pertains to calculation of the measured resistance of a carbon fiber cement column of size $426 \times 92 \times 76$ mm^3, as typical of a full-size structure. The specimen is divided into 31 027 elements in the FEM analysis.

The resistance is measured along the 426 mm length of the column. Only loop contacts and line contacts are considered, due to the relevance to the practical situation. A loop contact is perpendicular to the length of the column, such that it is around the 92 mm × 76 mm perimeter of the column. A line contact is a line perpendicular to the length of the column, such that it is on either the 92 mm wide surface or the 76 mm wide surface of the column. The contact resistance is taken into account. The unreal case in which the contact resistance is ignored is not considered in this section.

Figure 6 shows that the measured resistivity decreases monotonically with increasing distance between the adjacent voltage and current contacts, as in figure 5(b). The minimum distance between adjacent voltage and current contacts for accurate resistivity measurement is 50 mm in the case of loop contacts, and is 400 mm in the case of line contacts, as shown in figure 6. The results are close for the two sets of line contacts.

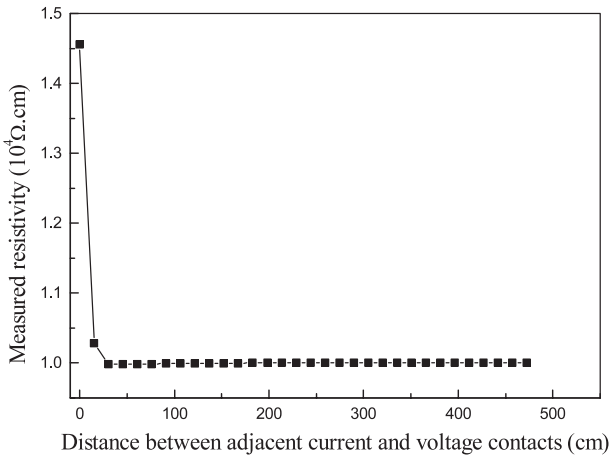

Figure 7. Dependence of the measured resistivity of a slab obtained by simulation on the distance between the adjacent voltage and current contacts.

3.4. Measured resistance of a slab

This section pertains to calculation of the measured resistance of a carbon fiber cement slab of size 384 × 192 × 12 in ($9.75 \times 4.88 \times 0.30\ m^3$), as typical of a full-size structure. The specimen is divided into 4096 elements in the FEM analysis.

The resistance is measured along the 9.75 m length of the slab. Only line contacts are considered, due to the relevance to the practical situation. Each line contact is along the 4.88 m width of the slab. The contact resistance is taken into account. The unreal case in which the contact resistance is ignored is not considered in this section.

Figure 7 shows that the measured resistivity decreases monotonically with increasing distance between the adjacent voltage and current contacts, as in figures 5(b) and 6. The minimum distance between adjacent voltage and current contacts for accurate resistivity measurement is 250 mm, as shown in figure 7. This distance is small compared to the value of 400 mm for line contacts in the case of the column of section 3.3. This is because of the small thickness of the slab compared to the cross-sectional size of the column.

3.5. Effect of the aspect ratio of a column

Consider a column of cross-sectional size 40 × 40 mm^2. Only loop contacts are used in this section. Let us calculate the effect of the aspect ratio (length of the column divided by 40 mm) on the measured resistivity. For each value of the aspect ratio, the measured resistivity approaches the true resistivity as the distance between the adjacent current and voltage contacts increases, as described in figure 5(b). The smaller is the aspect ratio, the less the measured resistivity approaches the true resistivity.

For each value of the aspect ratio, from a curve similar to figure 5(b), one can determine the maximum resistivity (which occurs when the distance between the adjacent current and voltage contacts is zero, i.e. the case of the two-probe method) and the minimum resistivity (which occurs at a non-zero distance between the adjacent current and voltage contacts, i.e. the case of the four-probe method). The ratio of the maximum resistivity to the true resistivity is called the

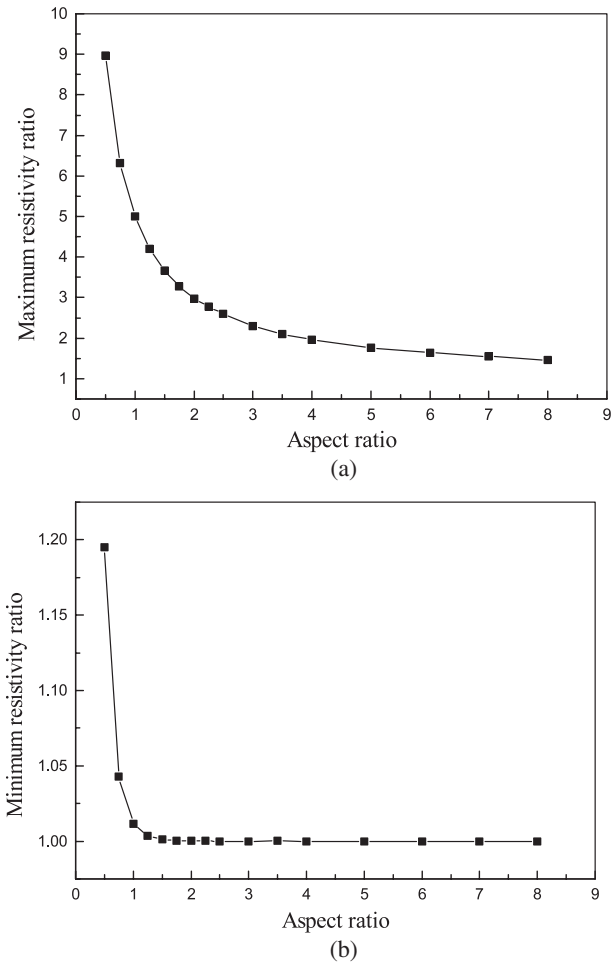

Figure 8. Dependence of the maximum (a) and minimum (b) measured resistivity of a column on the aspect ratio.

maximum resistivity ratio, which is shown in figure 8(a). The ratio of the minimum resistivity to the true resistivity is called the minimum resistivity ratio, which is shown in figure 8(b). The maximum resistivity ratio approaches 1 when the aspect ratio exceeds 8 (figure 8(a)). This means that the resistivity measured by using the two-probe method is accurate when the aspect ratio exceeds 8. The minimum resistivity ratio reaches 1 when the aspect ratio exceeds 1.5 (figure 8(b)). This means that the resistivity measured by using the four-probe method is accurate when the aspect ratio exceeds 1.5. Hence, for an aspect ratio less than 8, the four-probe method should be used.

Instead of considering the distance between the adjacent current and voltage contacts, one can consider the distance between the voltage contacts. For each value of the aspect ratio, the measured resistivity approaches the true resistivity as the distance between the voltage contacts decreases. The distance between the voltage contacts below which the measured resistivity is equal to the true resistivity is hereby called the critical length. The ratio of the critical length to the overall length of the column is hereby called the critical length ratio. The higher is the aspect ratio, the greater is the critical length ratio. For example, for an aspect ratio of 3.5, the critical length ratio is 0.8. Figure 9 shows that the aspect ratio must exceed 1.2 in order for the critical length ratio to be

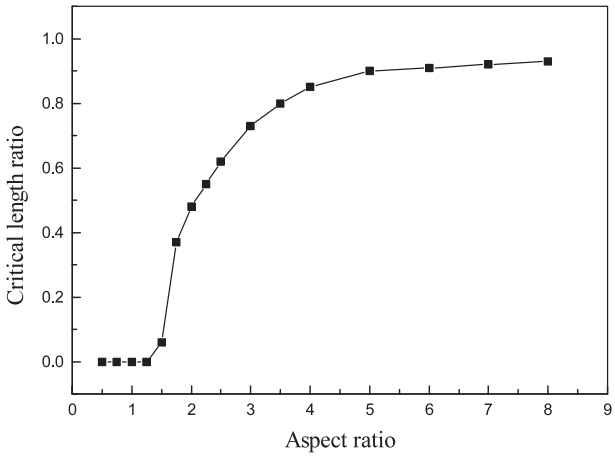

Figure 9. Dependence of the critical length ratio of a column on the aspect ratio.

non-zero. This means that the measured resistivity cannot be accurate when the aspect ratio is below 1.2.

Although a column of cross-sectional size 40 × 40 mm^2 was used in the above calculation, similar calculation involving different cross-sectional dimensions (other than 40 mm) but the same values of the aspect ratio was also conducted. It was thus found that the results shown in figures 8 and 9 concerning the effect of the aspect ratio are independent of the cross-sectional dimensions.

4. Conclusion

A finite element model for simulating the measurement of electrical resistance in carbon fiber reinforced cement is provided. The model allows calculation of the resistivity measured using different electrical contact configurations and specimen geometries, thereby allowing assessment of the effectiveness of various electrical contact configurations and providing a numerical tool for the design of the configurations for various specimen geometries and dimensions. It also allows calculation of the current density distribution.

The measured resistance using the four-probe method decreases with increasing distance between the adjacent voltage and current contacts. For a beam of size 320 × 40 × 40 mm^3, the minimum distance for accurate resistivity measurement by the four-probe method is 5 mm in the case of surface contacts (due to contact resistance), 5 mm in the case of loop contacts (due to contact resistance and non-uniform current density distribution) and is 40 mm in the case of line contacts (mainly due to the non-uniform current density distribution). The use of loop contacts is essentially as reliable as the use of surface contacts, although the current density is more uniform for surface contacts than loop contacts.

The resistivity measured by using the two-probe method is less accurate than that measured by using the four-probe method. It is highest (most inaccurate) for the line contacts and lowest (most accurate) for the surface contacts. This is due to the most severe current density nonuniformity for the case of the line contacts.

Using loop contacts, the two-probe resistivity measured along the length of a column is accurate when the aspect ratio exceeds 8, whereas the four-probe resistivity is accurate when the aspect ratio exceeds 1.5.

For a column of size 426 × 92 × 76 mm^3, the minimum distance between the adjacent current and voltage contacts for accurate resistivity measurement in the direction of the length of the column by the four-probe method is 50 mm in the case of loop contacts and 400 mm in the case of line contacts. For a slab of size 9.75 × 4.88 × 0.30 m^3, the minimum distance between the adjacent current and voltage contacts for accurate resistivity measurement in the direction of the longest side of the slab by the four-probe method is 250 mm in the case of line contacts.

References

[1] Chen P-W and Chung D D L 1995 Improving the electrical conductivity of composites comprised of short conducting fibers in a non-conducting matrix: the addition of a non-conducting particulate filler *J. Electron. Mater.* **24** 47–51
[2] Chung D D L 2004 Electrically conductive cement-based materials *Adv. Cem. Res.* **16** 167–76
[3] Chung D D L 2003 *Multifunctional Cement-Based Materials* (New York: Dekker)
[4] Chung D D L 2002 Piezoresistive cement-based materials for strain sensing *J. Intell. Mater. Syst. Struct.* **13** 599–609
[5] Wen S and Chung D D L 2003 A comparative study of steel- and carbon-fibre cement as piezoresistive strain sensors *Adv. Cem. Res.* **15** 119–28
[6] Wen S and Chung D D L 2005 Strain sensing characteristics of carbon fiber cement *ACI Mater. J.* **102** 244–8
[7] Wen S and Chung D D L 2006 Self-sensing of flexural damage and strain in carbon fiber reinforced cement and effect of embedded steel reinforcing bars *Carbon* **44** 1496–502
[8] Wen S and Chung D D L 2006 Effects of strain and damage on the strain sensing ability of carbon fiber cement *J. Mater. Civil Eng.* **18** 355–60
[9] Reza F, Batson G B, Yamamuro J A and Lee J S 2003 Resistance changes during compression of carbon fiber cement composites *J. Mater. Civil Eng.* **15** 476–83
[10] Wu B, Huang X and Lu J 2005 Biaxial compression in carbon-fiber-reinforced mortar, sensed by electrical resistance measurement *Cem. Concr. Res.* **35** 1430–4
[11] Yao W, Chen B and Wu K 2003 Smart behavior of carbon fiber reinforced cement-based composite *J. Mater. Sci. Technol.* **19** 239–43
[12] Shi Z-Q and Chung D D L 1999 Carbon fiber reinforced concrete for traffic monitoring and weighing in motion *Cem. Concr. Res.* **29** 435–9
[13] Wang S, Wen S and Chung D D L 2004 Resistance heating using electrically conductive cements *Adv. Cem. Res.* **16** 161–6
[14] Yehia S, Tuan C Y, Ferdon D and Chen B 2000 Conductive concrete overlay for bridge deck deicing: mixture proportioning, optimization, and properties *ACI Mater. J.* **97** 172–81
[15] Xie P and Beaudoin J J 1995 *Electrically Conductive Concrete and its Application in Deicing* (vol SP-154 *Advances in Concrete Technology*) (Farmington Hills, MI: American Concrete Institute) pp 399–417
[16] Tang Z, Li Z, Qian J and Wang K 2005 Experimental study on deicing performance of carbon fiber reinforced conductive concrete *J. Mater. Sci. Technol.* **21** 113–7
[17] Hou J and Chung D D L 1997 Cathodic protection of steel reinforced concrete facilitated by using carbon fiber reinforced mortar or concrete *Cem. Concr. Res.* **27** 649–56
[18] Wen S and Chung D D L 2007 Piezoresistivity-based strain sensing in carbon fiber reinforced cement *ACI Mater. J.* **104** 171–9
[19] Wen S and Chung D D L 2001 Cement-based controlled electrical resistivity materials *J. Electron. Mater.* **30** 1448–51